Section A -Research paper

Current Design of Rectangular Steel Silos: Limitations and Improvement

AlHussein Hilal[(1*)], A. M. Sanad[(1)], Mohamed H. Abdelbarr[(2)], Osman M. O. Ramadan[(2)], and Hany Abdalla[(2)]

[(1)] Department of Construction and Building Engineering, College of Engineering and Technology, Arab Academy for Science, Technology and Maritime Transport (AASTMT), 2033 Elhorria, Heliopolis, Cairo, Egypt;

[(2)] Department of Structural Engineering, Faculty of Engineering, Cairo University, 12613, Cairo, Egypt

***Corresponding author: AlHussein Hilal, E-mail:** alhusseinibrahim@aast.edu

Article History: Received: 05.08.2023 **Revised:** 11.08.2023 **Accepted:** 31.08.2023

Abstract

This study proposes a modification for the current design approach for rectangular silos that accounts for silos' wall flexibility. First, the authors investigated the effect of wall stiffness, symbolized by the wall width-to-thickness ratio (a/t), on the wall-filling pressure using a recently validated 3D finite element model (F.E.M.). The model was then employed to predict the pressures acting on flexible-wall silos accounting for the stress state in stored granular materials. Most design formulas and guidelines assume silos' walls to be rigid. However, this assumption is acceptable for the case of thick-wall concrete silos; it is questionable for thin-wall metal silos. Consequentially, it is crucial to determine the minimum wall stiffness necessary to secure the applicability of the current design rigid wall assumption, and to propose a way to deal with more flexible walls. To this end, several wall pressure distributions corresponding to filling steel silos with varied wall thicknesses were studied.

A new adjustment to the Janssen technique was proposed to better estimate the wall-filling pressures for square or rectangular silos. In the case of square silos, the Eurocode uses the Janssen equation and an equivalent radius of a corresponding circular silo (with the same hydraulic radius) to determine the wall pressure. This method predicts pressure values that are practically accurate for rigid-wall silos, but their accuracy decreases for flexible-wall silos. As a result, the Janssen equation was modified in this research to generate more accurate pressure estimates based on the equivalent volume concept. The finite element results of several developed models with the same granular material were compared to the estimations of the newly established approach to verify the broad range of its applicability.

Keywords: Silos, rectangular silos, filling pressure, silos design, Eurocode.

DOI: 10.48047/ecb/2023.12.8.798

1. Introduction

1.1. Background

Silo structures are utilized extensively in different sectors for storing and conveying granular materials in multiple activities such as; farming, mining, chemical, mineral processing, and energy areas [1–5]. Several studies have extensively studied the pressures exerted on circular silos since they are the most commonly used in different applications. However, fewer investigations were performed on square or rectangular silos [4,6].

Rectangular silos are advantageous over circular silos in terms of utilization and construction costs. However, structural analysis of

rectangular silo walls is more complicated since they are subjected to bending moments and membrane actions compared to circular silo walls, which are primarily subjected to membrane forces [7,8]. Furthermore, the structural behavior of rectangular wall silos depends primarily on the wall flexibility and the friction between the granular materials and walls [4].

Most classical theories for circular silos walls are based on the equilibrium of a horizontal strip of granular materials. The Janssen theory is one of the most widely used theories in design practices to predict wall pressure for circular silos [10-11, 13]. According to Jansen's theory, the mean wall pressure is only affected by the characteristics of the granular materials and the silo dimensions. However, it is considered constant, with no variations in the horizontal plan section of the silo. The Janssen approach had been extended to include non-circular silos by defining a square silo equivalent to a circular silo with the same hydraulic radius. This approximation was employed in most existing design codes and standards [11–13] to only anticipate the pressure applied on rigid silo walls. Eurocode detailed calculating the equivalent hydraulic radius for the square planform using the cross-sectional area (A) and circumference (U) of non-circular silos. This approach assumes that the silo wall is relatively stiff and that the lateral pressure ratio remains constant as silo altitude increases. Thus, there is a limitation to using the Jansen extended approach for designing flexible wall silos, which can be widely applicable to steel silos. Several scholars [14–20] have investigated square and rectangular silos and implemented various suggestions and concepts to demonstrate the discrepancies between the wall pressure variations acting on silo walls and Janssenian pressure.

The Janssen equation estimates the lateral wall pressure assuming that the wall pressure is constant at a specific silo's height. This assumption can be acceptable for circular silos since the circumference may experience homogeneous horizontal pressure distribution. Nevertheless, the lateral wall pressure for square silos is variable, especially at the corner section, resulting in a significant variance in the horizontal pressure distribution [7]. As a result, utilizing the existing approach for square silos based on the same hydraulic radius predicts inaccurate pressures acting on the silo walls, resulting in inadequate design and maybe failure. As a result, the current approach based on Jansen needs to be modified.

The optimal wall thickness for a square silo depends on the wall pressure value and distribution [8]. This study aims to address two problems: the varying pressure regimes that have arisen depending on wall thickness for several square silos using finite element modeling to provide structural design guidance; and a modification of the Janssen theory to provide a better prediction for the wall pressure acting on the silo wall, not the mean wall pressure.

1.2.Objective

The research developed a wall width-to-thickness ratio using a validated FEM and evaluated its effects on wall pressure, deformation, and load strength to provide Eurocode recommendations. This was done by raising wall thickness and maintaining other parameters constant until wall stiffness was reached. Set restrictions for wall width-to-thickness ratio change to provide silo designers options.

The FEM was also utilized to offer an update to the Janssen approach that improves wall pressure estimates for deep and flat silos. The suggested method employed the same volume concept for the actual silo and virtual circular planforms. In this context, the FEM confirmed and validated the new technique. Two aspect ratio silos were tested to

verify and generalize the newly developed technique to squat and slim silos.

2. Finite Element Model

2.1. FEM Validation

The FEM employed in this study to represent the granular materials is a continuum of elements with a nonlinear elastic-plastic constitutive law. The developed FEM was compared and validated using Lahlouh's experimental work at Edinburgh University [20,19,21] and the Janssen Formula [10]. Hilal et al. [4] have extensively detailed this validation process in their work. The pilot-scale model utilized in this research was developed using a 6 mm thick steel wall with a 1.5m square section (d) and a height (h) of 2.5m. It was filled with Leighton Buzzard sand, with a density of 1587 kg/m^3 [h/d= 1.67].

2.2.Model Description

The FEM was developed using ABAQUS software [22]. Due to symmetry, only one-quarter of the silo was, as shown in Figure 1. The silo model consists of three parts; the silo wall, the base, and the granular materials. Brick elements were chosen for modeling the silo walls, the base, and the granular materials (C3D8R).

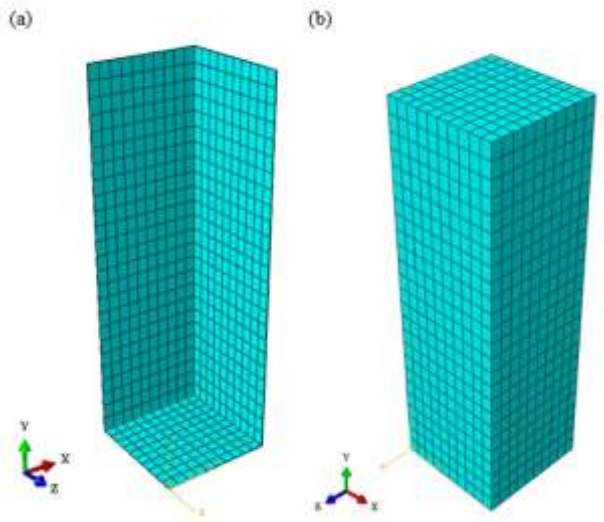

Figure 1. FEM: (a) base and wall elements; (b) bulk solids elements (sand).

2.3. Stored solids

The behavior of the bulk materials was simulated using an elastoplastic model based on the Drucker-Prager criterion [23], while the steel walls and base behavior were modeled using Hooke's law in the elastic zone and the plasticity criterion to identify the yield zone.

Leighton Buzzard sand was used in this study as the ensiled material. The characteristics of granular materials were derived from the experimental work of Lahlouh [19] and Goodey [8,23]. Tables 1 and 2 show the physical and mechanical parameters needed to define the constitutive law behaviors of bulk solids and steel, respectively.

Table 1. Properties of the bulk solids used in the FEM.

No.	Parameter	Value
1	Density, ρ (kg/m^3)	1587
2	Poisson's Ratio, ν	0.3164
3	Wall/ friction coefficient, μ	0.445
4	Internal angle of friction, β	45.1
5	Initial yield stress, $\sigma_{c\,o}$	0.25
6	Dilation angle, ψ	0

Table 2. Properties of the steel used in the FEM

No.	Parameter	Value
1	Density, ρ (kg/m^3)	7500
2	Poisson's Ratio, ν	0.3
3	Young's Modulus (GPa)	210
4	Yield stress (MPa)	240
5	Plastic strain	0

2.4.Bulk solid-silo wall interface

A contact pair option was used in the FEM to simulate the interaction between the silo wall and bulk solids. The FEM was modeled using the Coulomb friction model [4,8] to simulate the frictional interaction surface with a constant coefficient of friction (μ = 0.445). The penalty friction formulation was used for constraint enforcement, and the sliding formulation was finite sliding.

Several models with varying silo wall thicknesses [t_{wall} = 6, 10, 15, 30, 60 mm] were developed, with a constant wall width of 1.5 m and a fixed height of 2.5 m (see Table 3). The effect of changing the wall width-to-thickness ratio (a/t) versus numerous parameters was investigated using the developed models. The parametric study includes the wall-filling pressure distribution, maximum wall deformation, and percentage of transmitted vertical load to the silo wall.

Table 3. Wall width-to-thickness ratio for several analyzed squat silos with height (h) = 2.5 m, and width (a) =1.5 m.

Silo No.	**1**	**2**	**3**	**4**	**5**
Wall thickness, t (mm)	6	10	15	30	60
Wall width-to-thickness ratio "a / t"	250	150	100	50	25

It is important to mention that all FEMs had a flat base vertically constrained in the Y-direction. To prevent normal displacements regarding the symmetry plane, the boundary conditions of the silo walls and granular materials were only established around the axis of symmetry in the x and z directions, as shown in Figure 2.

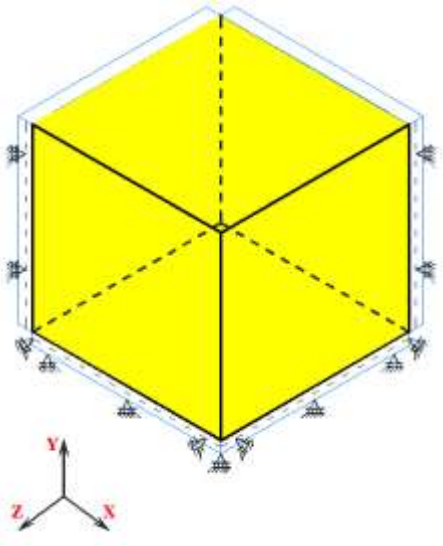

Figure 2. Assignment of boundary conditions for a quarter silo

3. Results

3.1. Wall-filling pressure

The wall-filling pressures were measured in vertical and horizontal projections to observe the wall pressure distribution imposed on the silo wall, as shown in Figures 3 and 4. Figure 3 shows three vertical sections of the silo wall obtained at the middle, quarter and corner for the various wall width-to-thickness ratios to highlight the variation of wall-filling pressures throughout the silo height and compare them to a silo with rigid wall analysis.

Figure 4 shows the horizontal distributions of wall pressures over the full length of the silo wall. The wall width-to-thickness ratio (a/t), as illustrated in Figures 3 and 4, considerably influences the distribution of lateral pressure acting on the wall. As the width-to-thickness ratio of the wall increases, the wall's behavior becomes more rigid, and wall pressure is redistributed from the corner to the center due to the increased wall stiffness. This process was repeated until the pressure distributions across the wall seemed to be almost uniform.

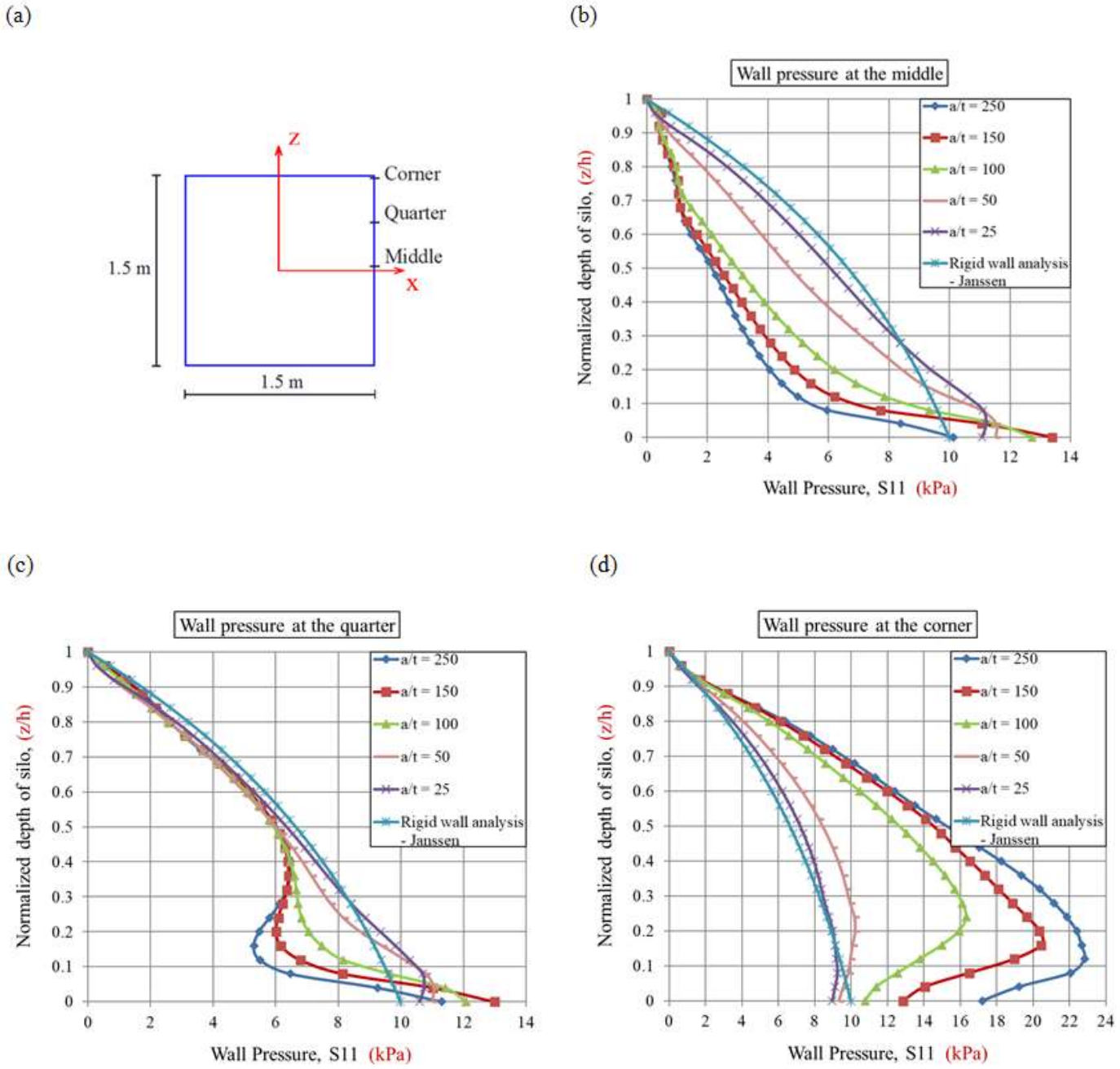

Figure 3. Wall-filling pressures for various wall width-to-thickness ratio models,
(a) square silo cross-section sketch, (b) at the middle, (c) at the quarter, (d) at the corner [h/a= 1.67]

Consequently, determining the wall width-to-thickness ratio at which the wall would act like a rigid is critical for establishing the stiffness limitations.

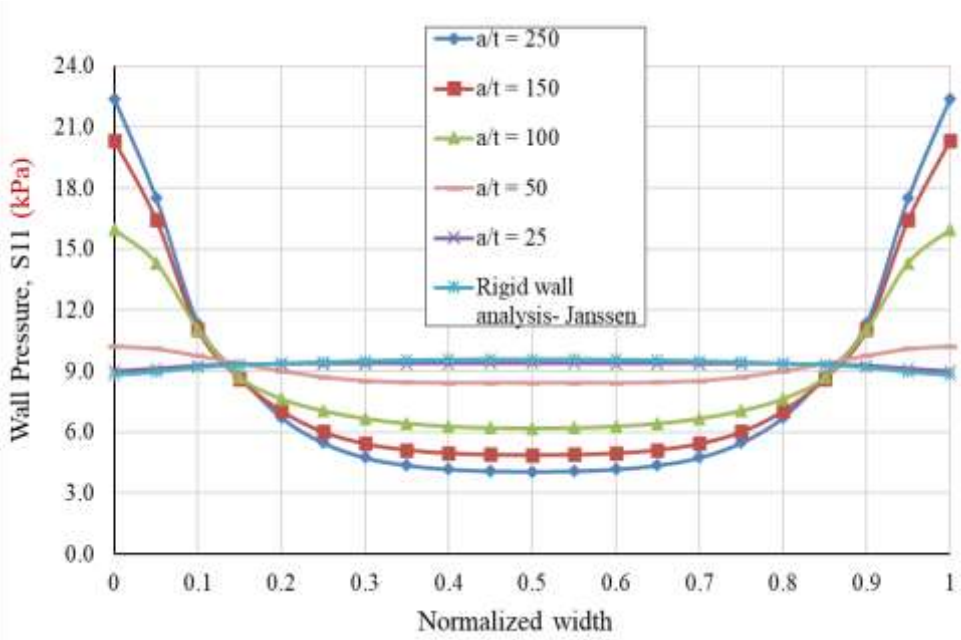

Figure 4. Effect of wall width-to-thickness ratios on lateral wall pressure above the base by 0.5 m (20% of the silo height).

The different wall width-to-thickness ratio was used to assess whether the wall is rigid or flexible. From Figures 3 and 4, it can be seen that a stiffness ratio of 25 describes a completely rigid wall. The same conclusions can be seen in Figures 4 and 5. A wall width-to-thickness ratio of 50 leads to a close value of wall pressures for the rigid case.

Figure 5 describes the relationship between the wall width-to-thickness ratio and the lateral wall pressure at the mid-span of the silo wall in order to obtain the minimum required wall width-to-thickness ratio for achieving conservative wall rigidity behavior, as shown in Figure 4. The selection of wall pressure at mid-span results from the sensitivity of the flexible wall in that region.

The wall pressures for wall width-to-thickness ratio models were measured at 20% of the silo's height from the base to solely examine the effect of the wall width-to-thickness ratio and avoid the effect of boundary conditions. The end effects have already been reported in previous studies. [4,7].

The conservative wall width-to-thickness ratio (a/t) was recommended to accomplish 90% of the wall-filling pressures of a rigid wall condition. Figure 6 shows a horizontal line intersecting the graph line at 90% of the pressure value, which is then dropped vertically to get the relevant wall width-to-thickness ratio.

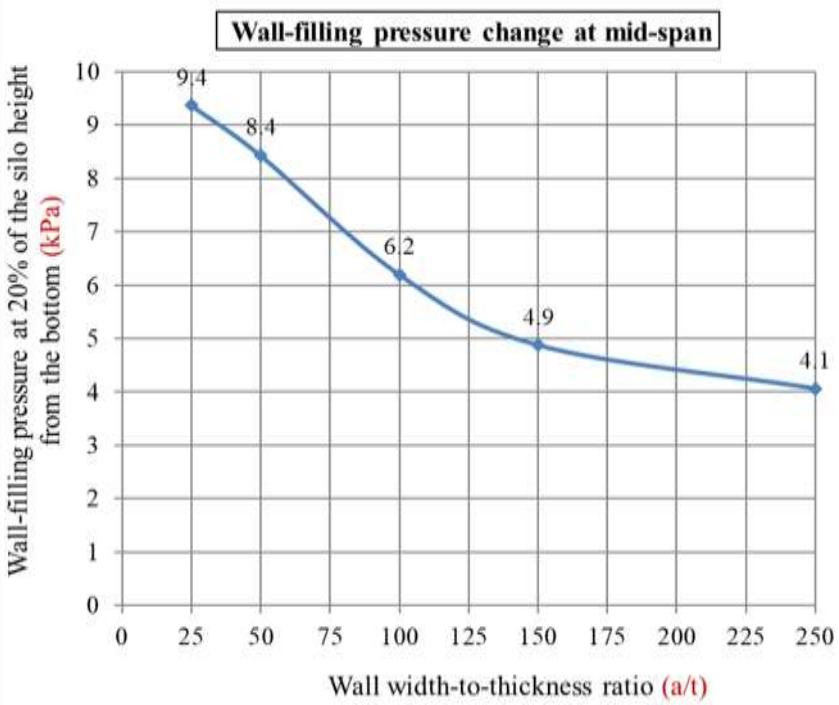

Figure 5. Wall-filling pressures with various wall width-to-thickness ratios (a/t).

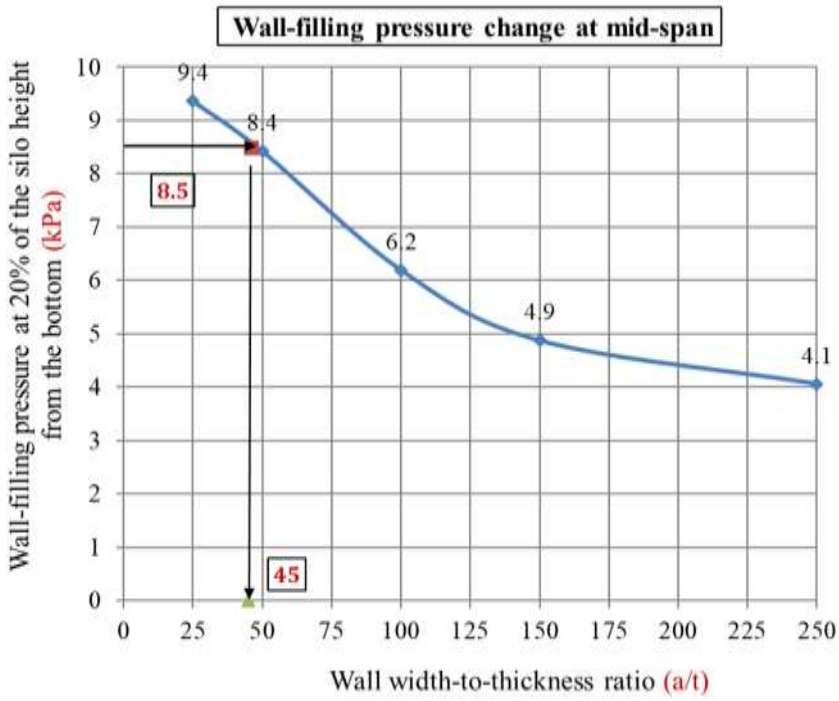

Figure 6. Estimating the conservative wall width-to-thickness ratio for 90% of rigid wall case (a/t = 45).

Since the relevant wall width-to-thickness ratio for 90% of rigid walls was 45, the minimum wall thickness is 34 mm. Two further checks were performed to claim that the wall's behavior will be relatively rigid: the maximum deformation and capacity load of these walls.

3.2. Maximum deformation

Several assumptions are made while applying the Eurocode to estimate wall pressures for silo walls. One of these assumptions is that the wall is rigid [6], indicating that no deformations have occurred. As a result, the actual wall deformations must be in that manner or within code limitations at the recommended conservative wall width-to-thickness ratio. The Eurocode (1993-4-1) [24] specifies the global lateral deflection limitation value as the lesser of the:

$$\boldsymbol{\delta_{max}} = \boldsymbol{k_1 H} \qquad \textit{Equation 1}$$

$$\boldsymbol{\delta_{max}} = \boldsymbol{k_2 t} \qquad \textit{Equation 2}$$

Where;

H: The structure's height from the base to the roof.

t: the wall's thinnest plate thickness.

k_1= 0.02 and k_2= 10 are recommended values.

H = 2.5 m (silo wall, flat-bottom end condition)

t = 0.034 m. (the suggested wall thickness)

$\boldsymbol{\delta_{max}}$ = 0.02 x 2.5 = 0.05 m.

$\boldsymbol{\delta_{max}}$ = 10 x 0.034 = 0.34 m.

Then the allowable $\boldsymbol{\delta_{max}}$ for the silo wall was 0.05 m = 50 mm.

Figure 8 shows the maximum lateral displacement of the silo wall versus the wall width-to-thickness ratio. The maximum wall deformation occurred in the center of the silo wall, according to EN1991-4 [25]. The relevant deflection of the conservative wall width-to-thickness ratio should be smaller than the limiting value specified by the Eurocode's limit to be accepted.

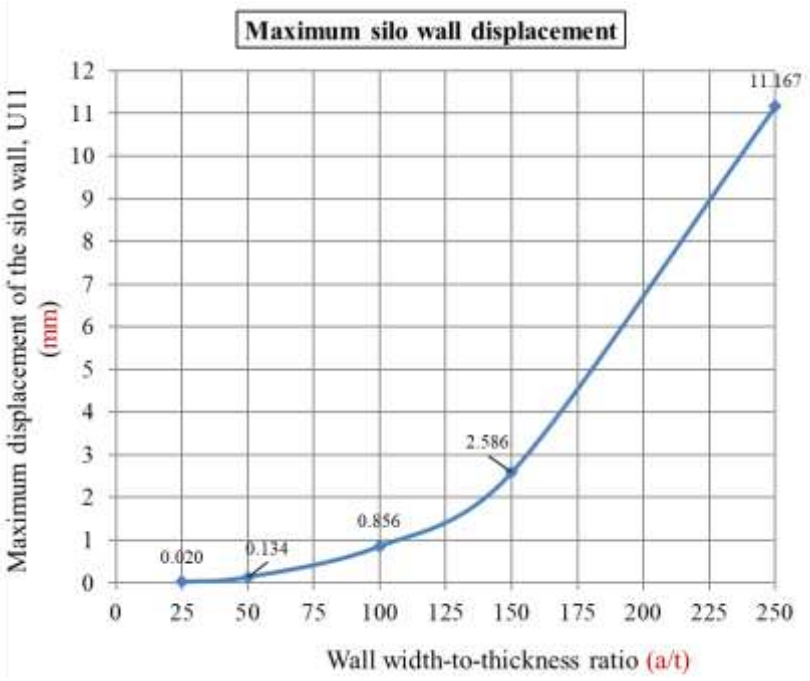

Figure 7. Wall deformation as wall width-to-thickness ratios (a/t) change

The wall deformation for a wall width-to-thickness ratio of 45 is about 0.10 mm. Consequently, the proposed wall width-to-thickness ratio fulfills the code requirement of 50 mm. As a result, using the code to solve these unstiffened silos is a good decision.

3.3.Vertical load distribution

The total vertical loads are induced by the weights of the granular materials and the structure's own weight. The silo's base and vertical walls sustain the vertical loads. A portion of the granular loads are transferred to the silo s walls in the vertical direction by frictional traction. This portion is highly dependent on the wall's rigidity. The vertical load sustained by the wall decreases as the rigidity decreases, and vice versa [4, 26]. As a result, it is important to compare the proposed

wall width-to-thickness ratio with the Eurocode requirement.

As seen in Figure 9, the percentage of vertical load due to own weight and granular material sustained by the wall decreases as the width-to-thickness ratio of the wall increases. Figure 10 provides the suggested percentage of vertical load distribution using a wall width-to-thickness ratio of 45. Consequently, the estimated percentage for the proposed wall width-to-thickness ratio is 56%.

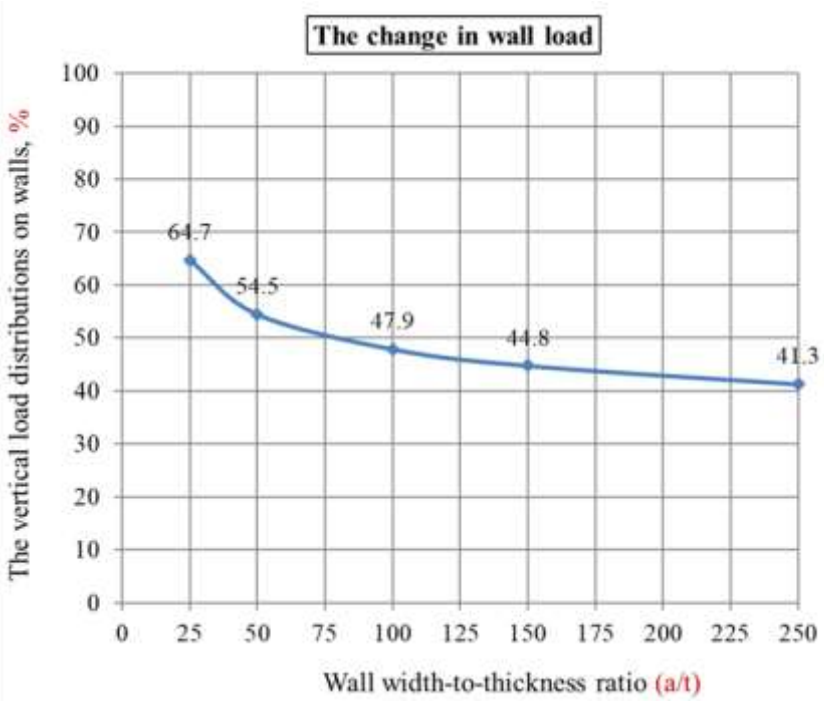

Figure 8. The vertical load distribution on walls with various width-to-thickness ratios (a/t)

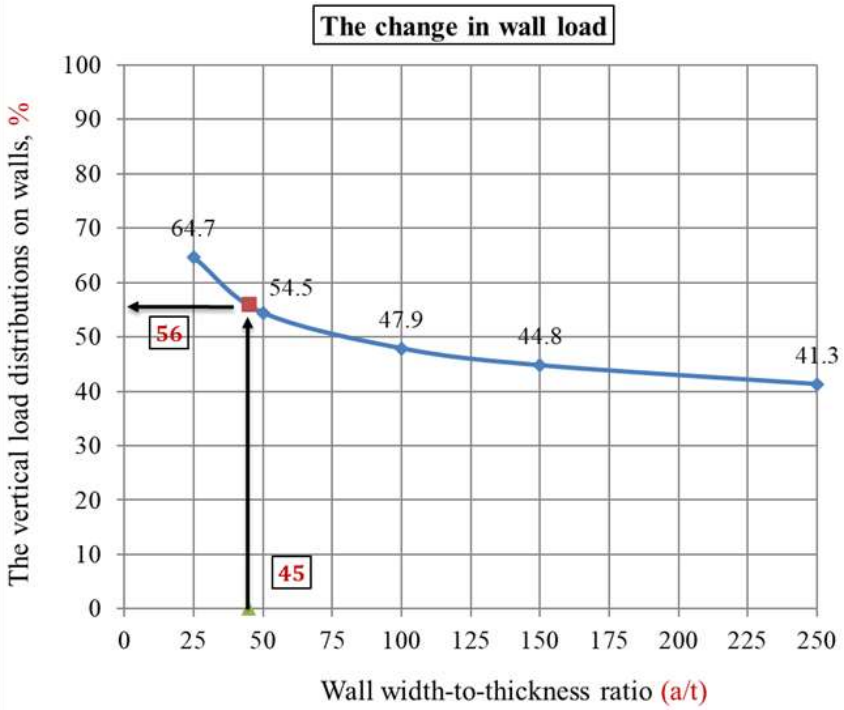

Figure 9. Estimating the vertical load distribution for the proposed wall width-to-thickness ratio (a/t) of 45

To ensure that the proposed wall width-to-thickness ratio complied with the Eurocode, the percentage of vertical force transferred to the wall was analytically calculated using the Janssen method [11] and compared to the predicted percentageThe vertical load carried by the wall at the proposed wall width-to-thickness ratio (56%) is more than the vertical load sustained by the wall if it is assumed to be a rigid wall case (45.6%). As a result, the proposed wall width-to-thickness ratio fulfills the third criterion for stiff wall analysis. Consequently, the codes can be applied to predict the wall-filling pressure for unstiffened steel walls when the wall width-to-thickness ratio ($a/t \leq 45$) is equal to or less than 45. Table 4 displays the tabulated results of several models with varied wall width-to-thickness ratios, including the three criteria used in this investigation.

3.4.Comparisons with rigid wall analysis

The primary results were summarized in three categories to propose a simplified design strategy for the flexible square planform silo.

- The wall width-to-thickness ratio is equal to or less than 25 ($a/t \leq 25$)

The wall will act as a completely rigid wall. As a result, the Eurocode can be used to predict the wall-filling pressure for silo walls.

- The wall width-to-thickness ratio ranges from 25 to 45 ($25 < a/t \leq 45$)

The wall-filling pressure varies within 10% of the rigid wall analysis at most. However, using the Eurocode is still a conservative approach for this proposed wall width-to-thickness ratio since the wall deformations and vertical load capacity are within acceptable limits, as shown in Table 4.

- The Wall width-to-thickness ratio exceeds 45 ($a/t > 45$)

As illustrated before, the silo wall will be categorized as flexible, and design code output will not provide an optimal design due to circular rigid wall assumptions. In this case, the authors propose an updated approach using a FEM considering wall deformability, bulk solid / structure interaction, failure mechanism, and wall imperfection [4].

Table 4. Summary of FEM analysis output for variable wall width-to-thickness ratios (a/t).

No.	a (m)	Wall thickness, t (m)	Height (m)	Wall width-to-thickness "a/t"	Wall filling pressure at 20% of silo height (kPa)	Maximum silo wall deformation (mm)	Vertical wall load %
1	1.5	0.006	2.5	250	4.1	11.167	41.3
2	1.5	0.01	2.5	150	4.9	2.586	44.8
3	1.5	0.015	2.5	100	6.2	0.856	47.9
4	1.5	0.03	2.5	50	8.4	0.134	54.5
5	1.5	0.033	2.5	45	8.5	0.100	56
6	1.5	0.06	2.5	25	9.4	0.020	64.7
7	1.5	Rigid Analysis (Janssen approach)	2.5	—	9.5	0	45.7

3.1.Proposed Modification to the Janssen Equation

For designing square silos, the Eurocode applies the Janssen equation to determine the wall pressure and radius of a comparable circular silo with the same hydraulic radius [11]. This approach predicts pressure values that are close to the mean lateral wall pressure of each level [8]. A prediction of a mean pressure value clearly underestimates pressure in certain areas while overestimating pressure in others [4]. All standards prohibit underestimating the actual applied loads and pressures on silo walls, which results in poor design approaches.

The Janssen equation was modified to provide more accurate pressure predictions for square silo walls. This prediction may provide a more realistic estimate of wall-filling pressure along the silo height, reducing the discrepancy between underestimating and overestimating when compared to finite element results. The proposed new approach uses a circular silo with the same volume as a square silo. The results showed that the proposed approach gives a more accurate estimation compared to standard code practices, including ACI and Eurocode, in estimating the wall-filling pressure for both rectangular silo walls.

One main drawback of using the Janssen method is neglecting the square section's corners when considered a circular section, as illustrated in Figure 10. This approach will result in an inaccurate design by reducing the imposed wall loads on the silo walls. As a consequence, as demonstrated in Figure 11, a new approach must be developed to address this issue and give a better alternative.

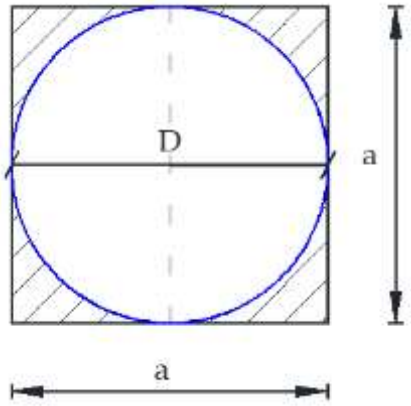

Figure 10. Example of square section and equivalent circular silo (existing approach)

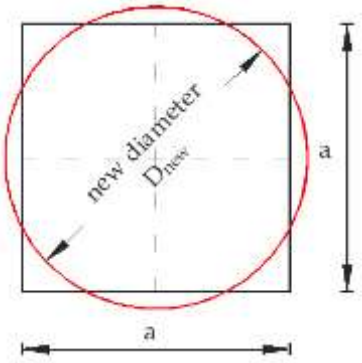

Figure 11. The suggested new equivalent circular cross-sectional area, $D_{new} = \sqrt{\frac{4A}{\pi}}$

The finite element results of the developed models were compared to the estimates of the proposed approach to provide a comprehensive methodology of the method's broad range of applications. This confirmation contains various vertical and horizontal section cuts showing the lateral wall pressures across the silo wall. A vertical section of lateral wall pressure was observed in the middle of the silo wall. Nevertheless, the horizontal section was obtained 0.5 m above the base.

Based on the previously validated model [4], the confirmation procedure used two distinct slenderness ratio models: squat and slender. The ensiled material for both silo models was Leighton Buzzard sand, with one adjustment that modified the behavior of the silo wall to rigid.

3.1.1. Squat model [h/a= 1.67]

The model's geometry was specified above in the model description section. Figure 12 shows the cross-sectional dimension of the square silo.

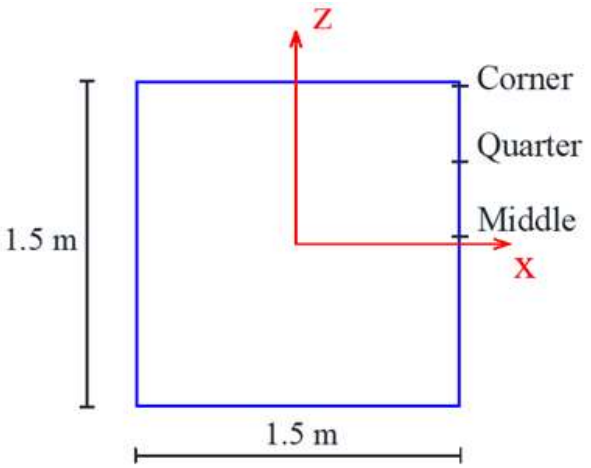

Figure 12. Squat silo sample with a 2.5-meter height [h/a = 1.67]

The modification will be carried out in the following steps:

- Calculate the diameter of the new equivalent circle with the same cross-sectional area as the square silo.

$$D_{new} = \sqrt{\frac{4A}{\pi}} \qquad \textit{Equation 3}$$

$$D_{new} = \sqrt{\frac{4x\ 2.25}{\pi}} =$$

1.692 m

- Calculate the "$R_{h,\,new}$" hydraulic radius for the newly created circular section.

$$R_{h,\,new} = \frac{D_{new}}{4} \qquad \textit{Equation 4}$$

$$R_{h,\,new} = \frac{1.692}{4} =$$

0.423 m

- Apply the Janssen equation using the new hydraulic radius, $R_{h,\,new}$.

$$P_x = \frac{R_{h,new} \cdot \omega}{\mu} \left(1 - e^{-\frac{1}{R_{h,new}} \cdot \lambda \cdot \mu \cdot Z}\right)$$

- New Hydraulic Radius, $R_{h,\,new}=D_{new}/4=$ 0.423m.
- Lateral pressure ratio for sand, λ = 1.1 (1- Sin 35.4˚)= 0.4628
- The specific weight of the material=1587kg/m^3
- Characterized depth, Z= 2.5 m.

$$\boldsymbol{P_x} = 10.62 \text{ kPa}$$

(a)

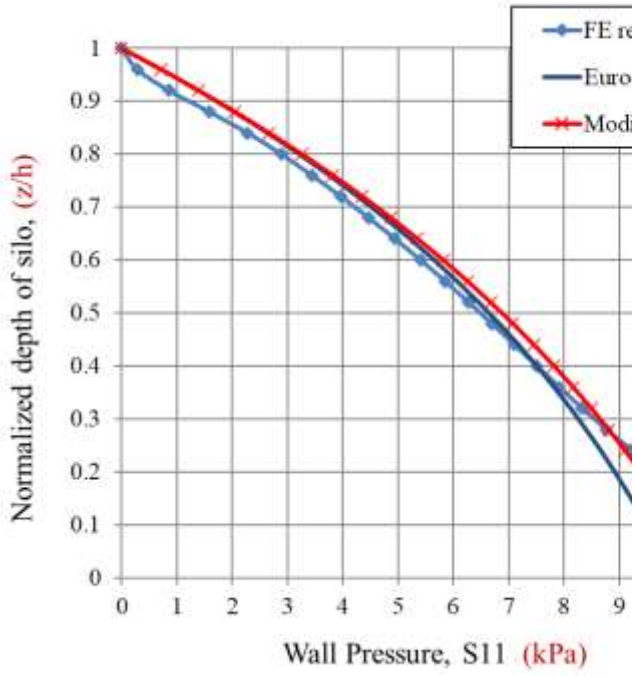

(b)

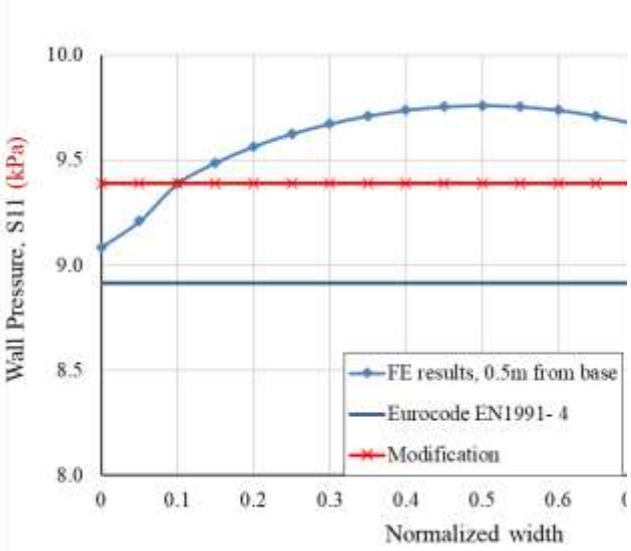

Figure 13 compares the lateral wall pressure between the finite element results, the Eurocode, and the proposed approach (the modification to the Janssen equation with the modified hydraulic radius) for the newly developed cross-sectional area. The new approach provides pressure estimates that match closely with FEM estimation of lateral wall pressure compared to the existing approach in Eurocode. Figure 14 compares the proposed Janssen approach update, the current Eurocode approach, and the finite element results.

(a)

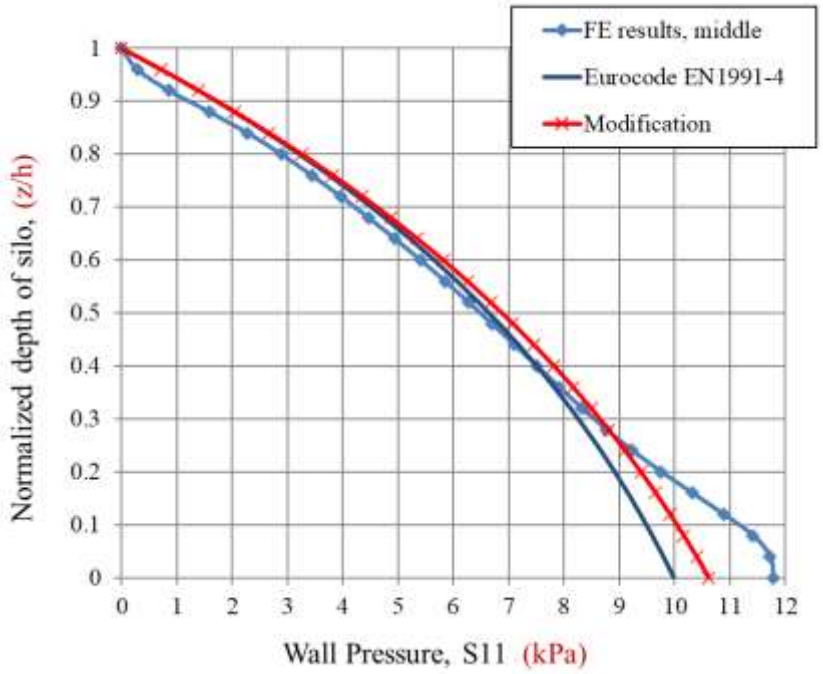

(b)

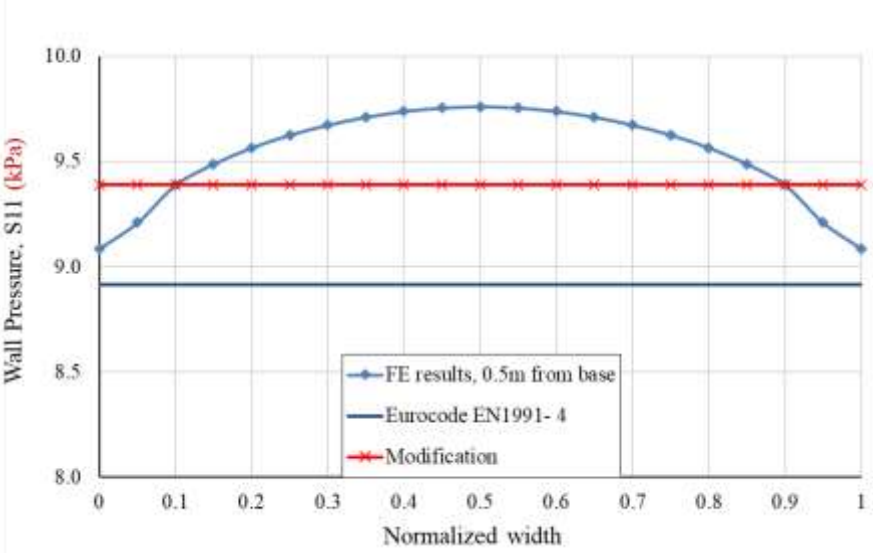

Figure 13. Comparison of different lateral wall pressures in the squat silo, (a) at the middle, (b) above the base by 0.5m [h/a= 1.67]

For the three vertical sections, neither the values of the modification nor the current method change. The FE results, on the other hand, differ, indicating that the proposed modification to the Janssen method better predicts the wall-filling pressure in squat silos.

(a)

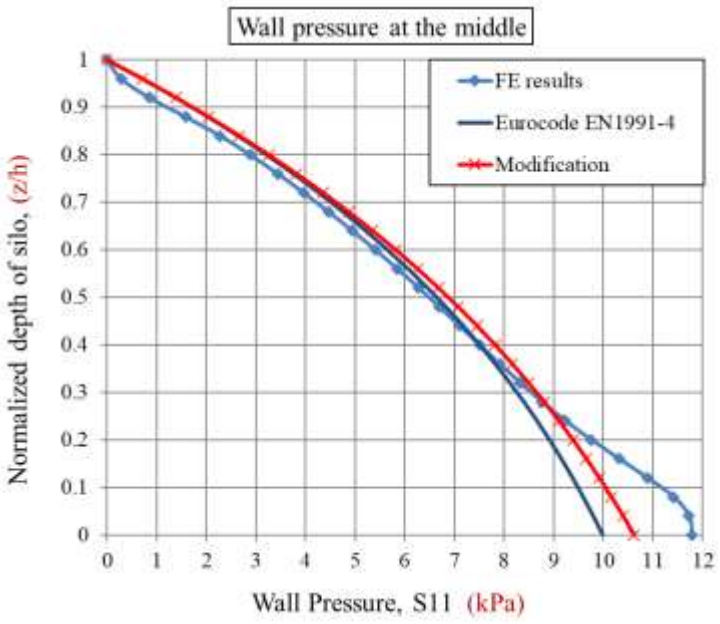

(b)

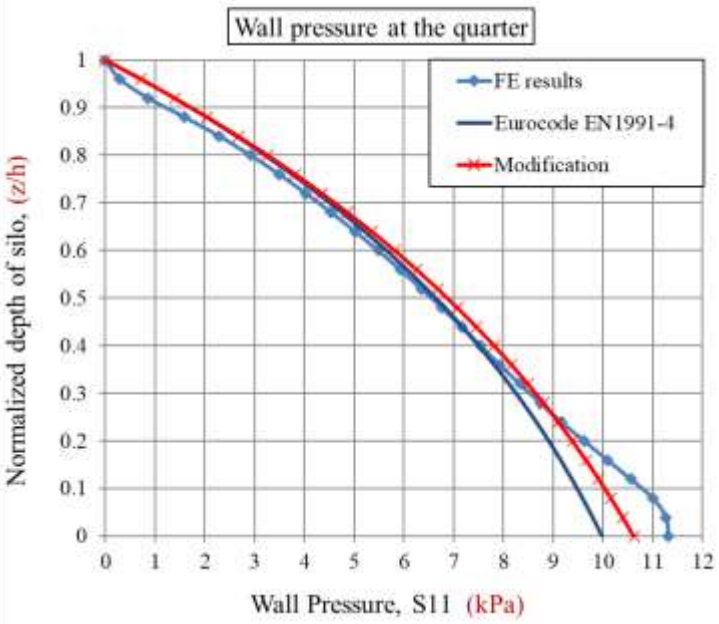

(c)

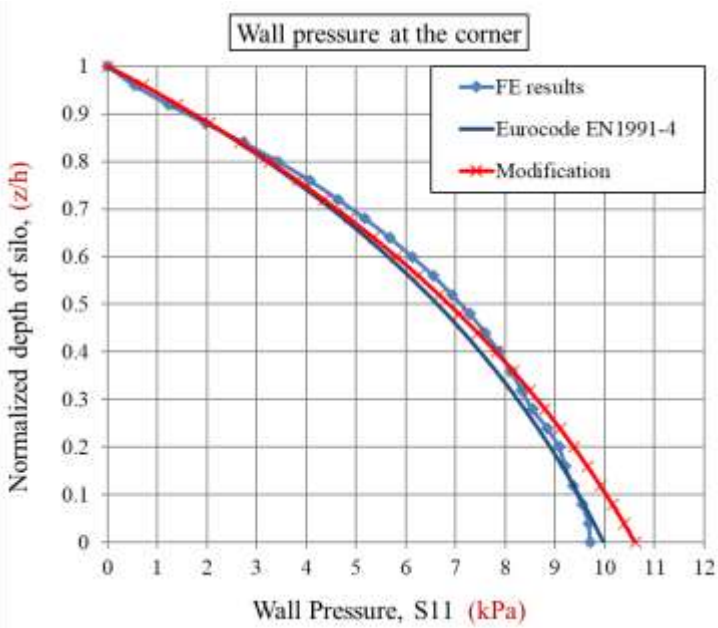

Figure 14. Comparison of the modified Janssen approach, the current Eurocode approach, and the FE results, (a) at the middle, (b) at the quarter, (c) at the corner [h/a= 1.67]

Figure 15 shows the difference between the proposed and the existing approach in percentage concerning the normalized depth of the silo. This normalized difference percentage is constant to the full width of the silo wall due to the assumption of uniform Janssenian pressure.

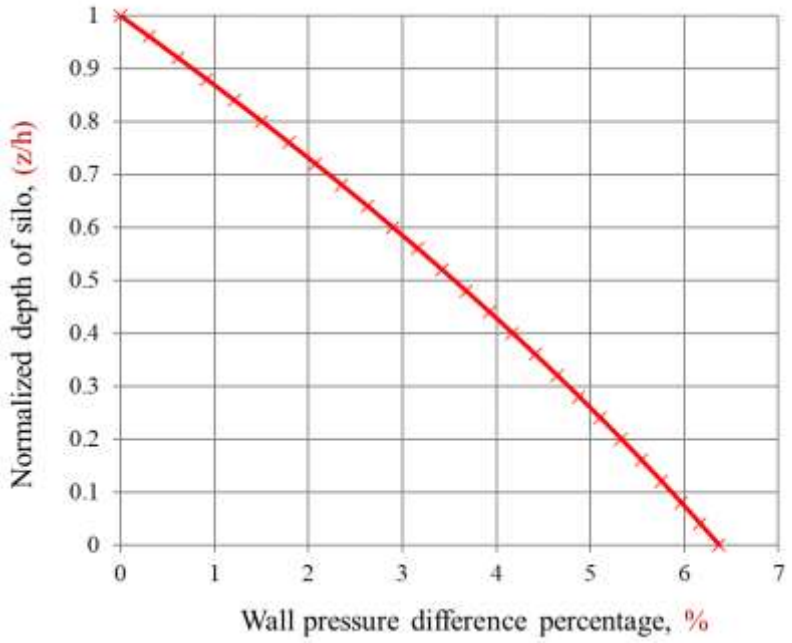

Figure 15. The normalized difference percentage of wall pressure between the modified and the existing Eurocode approaches for a squat silo

The normalized difference percentage is not uniform throughout the silo height, indicating that the modified and existing methods have values that are relatively close in the center of the silo and nearly identical at the top. The discrepancy, however, peaked near the silo's bottom. This is a positive sign since the FE yields the highest wall pressure in that region.

The vertical load transferred to the wall for both approaches was measured and tabulated, as shown in Table 5. This comparison aims to illustrate the changes in the transferred load to the walls using the parameters in Section 3.5.1 for the proposed approach. The compressive vertical loads on the wall in the proposed approach are approximately 4% less than the existing one, which may reduce the wall thickness estimation. This difference in vertical loads is directed to the silo base in the case of a flat-bottomed condition or to the hopper in the case of a hopper-end situation. The steps for calculating the following terms are illustrated in Section 3.3 in detail.

Table 5. Comparison of the vertical loads transferred to the walls by the two approaches

No.	Parameter	The existing approach	The proposed approach
1	The hydraulic radius, R (m)	0.375	0.423
2	the specific weight of the material, ω (kg/m^3)	1587	1587
3	Wall friction coefficient, μ	0.445	0.445
4	The lateral pressure ratio, λ	0.4628	0.4628
5	The depth from the free surface, Z (m)	2.5	2.5
6	The maximum lateral wall pressure, $\boldsymbol{Px}$ (kPa)	9.985	10.62
7	The maximum vertical pressure on the base, $\boldsymbol{P_v}$ (kPa)	21.6	22.95
8	Total vertical loads (Bulk solids, kN)	89.3	89.3
9	The vertical load on the base (kN)	48.6	51.63
10	The vertical load supported by the silo wall (kN)	40.7	37.67
11	The percentage of the transferred load to the wall	45.6 %	42.2 %

3.1.2. Slender model [h/a= 2.5]

Figure 16 illustrates the slender model cross-section with a dimension of 6.42 meters and a height of 16 meters, filled with the same granular material (sand).

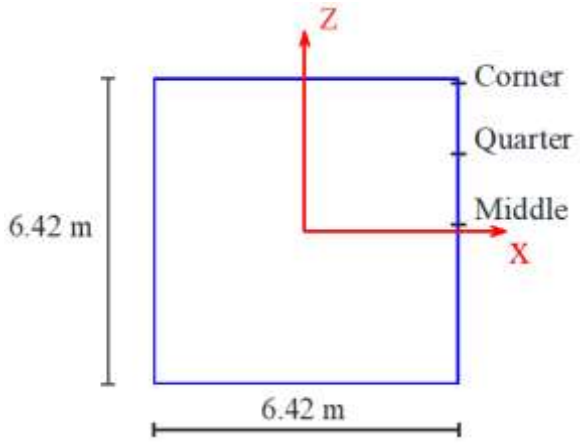

Figure 16. Slender silo cross-section with a 16-meter height [h/a = 2.5]

The modification will be carried out in the following steps:

- Calculate the diameter of the new equivalent circle with the same cross-sectional area as the square silo.

$$D_{new} = \sqrt{\frac{4A}{\pi}}$$

$$D_{new} = \sqrt{\frac{4x\ 41.2164}{\pi}} = 7.244 \text{ m}$$

- Calculate the "$R_{h,\ new}$" hydraulic radius for the newly created circular section.

$$R_{h,\ new} = \frac{D_{new}}{4}$$

$$R_{h,\ new} = \frac{7.244}{4} = 1.811\text{m}$$

- Apply the Janssen equation using the new hydraulic radius, $R_{h,\ new}$.

$$P_x = \frac{R_{h,new}\ .\ \omega}{\mu}\ (1 - e^{-\frac{1}{R_{h,new}} \cdot \lambda \cdot \mu \cdot Z})$$

- New Hydraulic Radius, $R_{h,\ new} = D_{new}/4 = 1.811$ m.
- Lateral pressure ratio for sand, $\lambda = 1.1$ (1- Sin 35.4˚)= 0.4628
- The specific weight of the material = 1587 kg/m^3
- Characterized depth, Z= 16 m.

$$\boldsymbol{P_x} = 54.11 \text{ kPa}$$

Figure 17 compares lateral wall pressure between the finite element results, the Eurocode, and the modification to the Janssen equation with the adjusted hydraulic radius for the newly developed cross-sectional area. The new approach closely matches the finite element results compared to the approach applied in Eurocode. It can be seen from Figure 17b that the proposed approach gives maximum values close to FEM results.

(a)

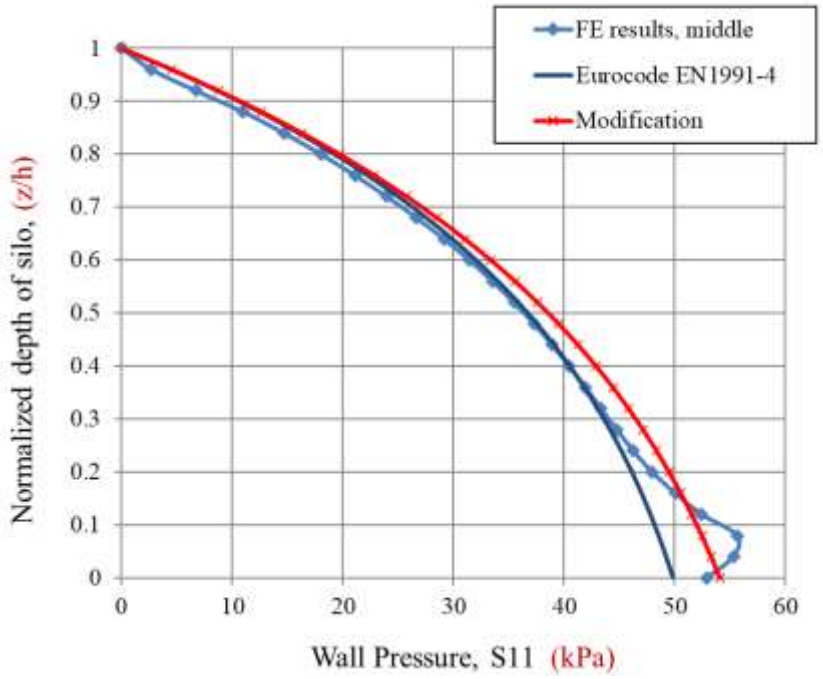

(b)

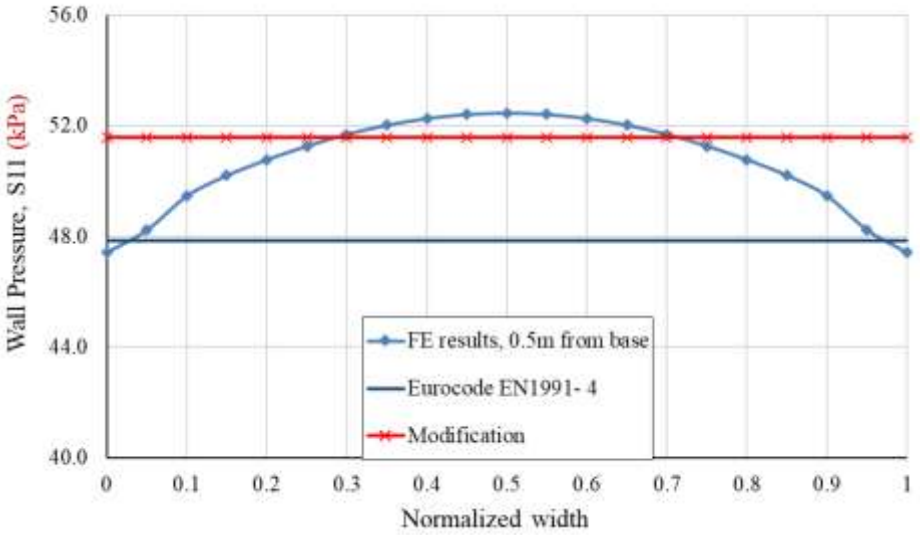

Figure 17. Comparison of different lateral wall pressures in the slender silo, (a) at the middle, (b) above the base by 0.5 meters [h/a= 2.5]

(a)

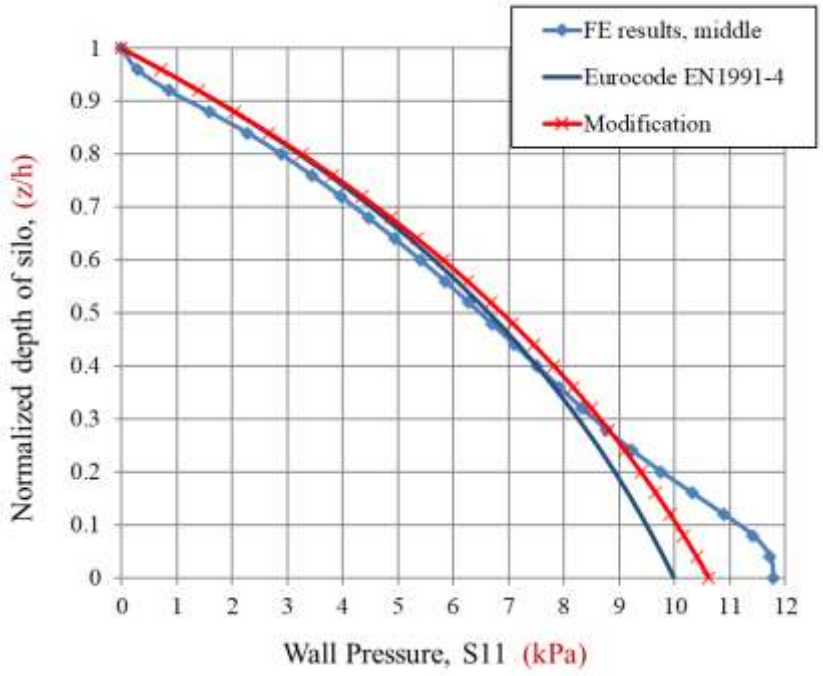

(b)

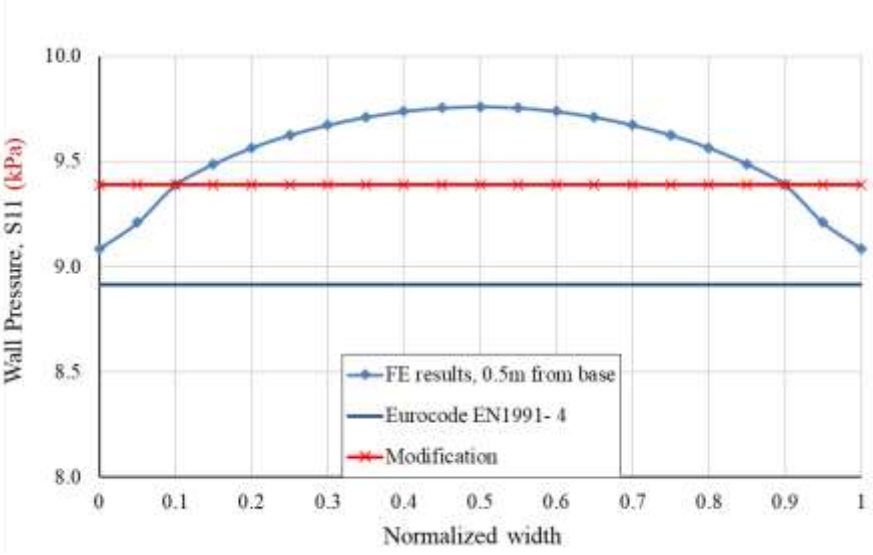

Figure 13 and Figure 17 show that the proposed approach provides better estimates compared to the current Eurocode method in predicting the maximum lateral wall pressure for squat and slender silos. Since the goal of implementing codes and standards is to give the actual pressure acting on the silo walls for the design process, which the current approach cannot provide.

As a result, designers can benefit from the results of this research to update design codes.

Error! Reference source not found. compares the proposed Janssen approach update, the current Eurocode approach, and the FEM outputs. It can be seen from **Error! Reference source not found.** that the proposed approach provides results that closely match the FEM model, especially for the maximum pressure values. Thus, the proposed approach better predicts the wall-filling pressure in slender silos.

(a)

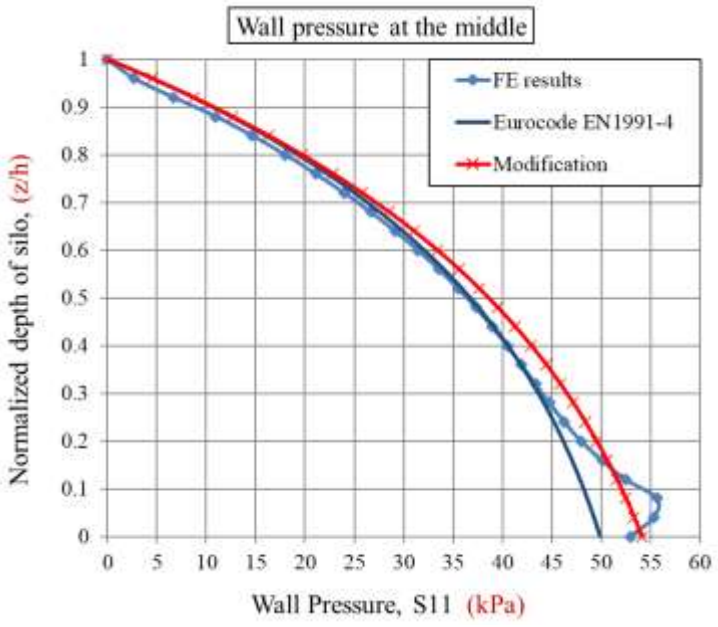

(b)

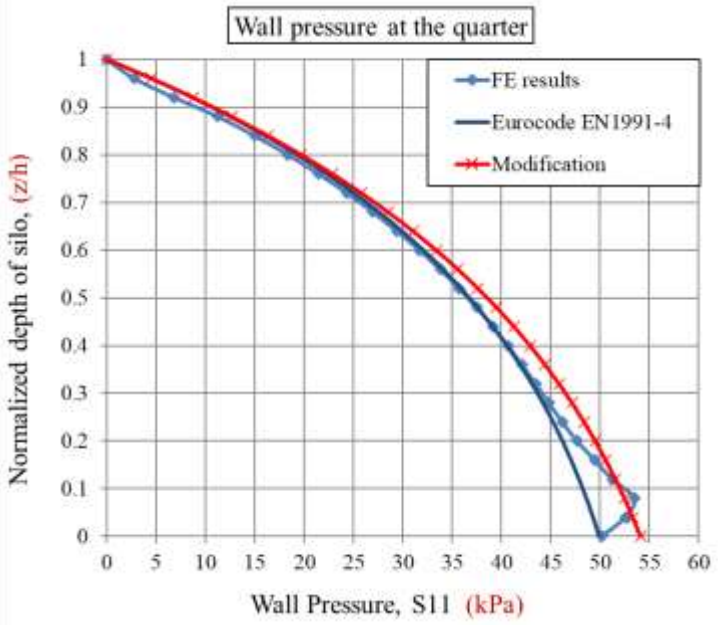

(c)

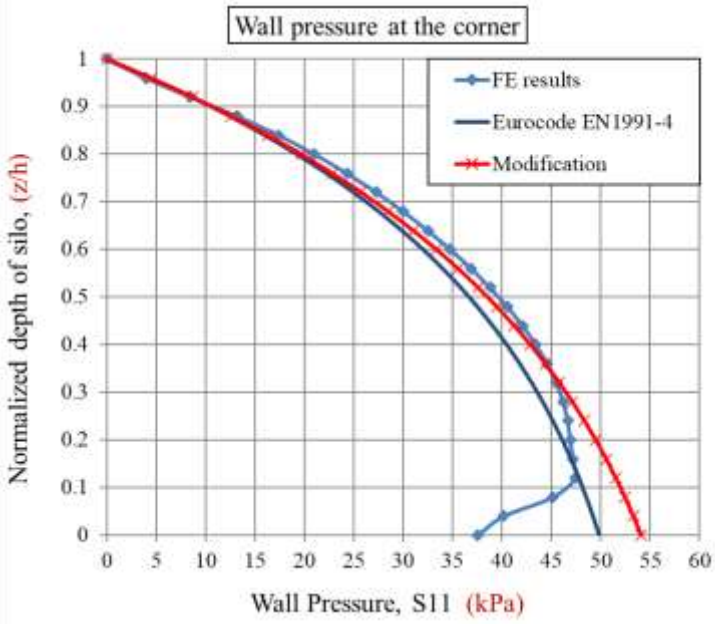

Figure 18. Comparison of the modified Janssen approach, the current Eurocode approach, and the FE results, (a) at the middle, (b) at the quarter, (c) at the corner [h/a= 2.5]

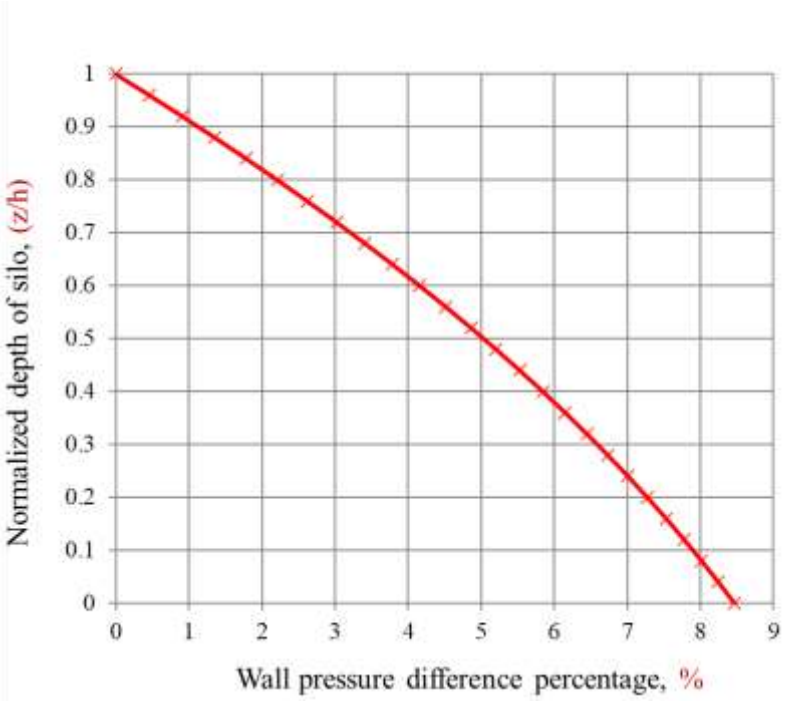

Figure 19 illustrates the percentage difference between the proposed and current approaches regarding silo normalized depth for the slender silo.

Both Figure 15 and

(a)

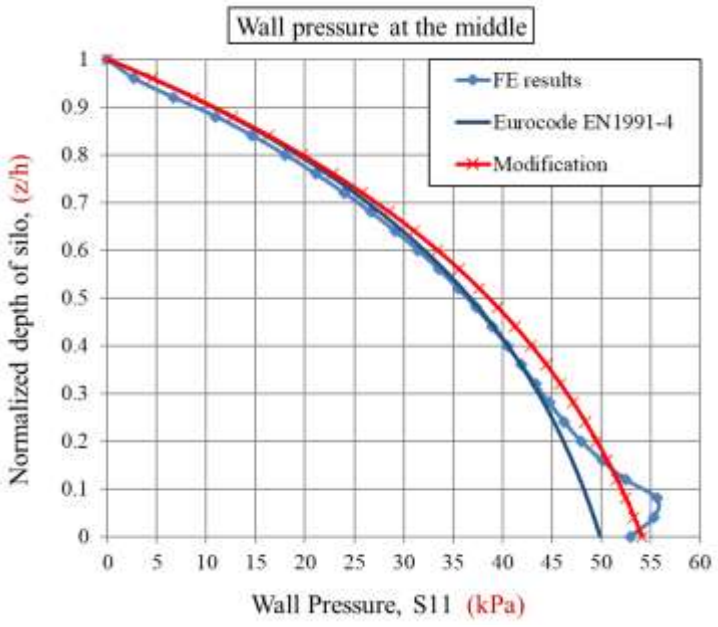

(b)

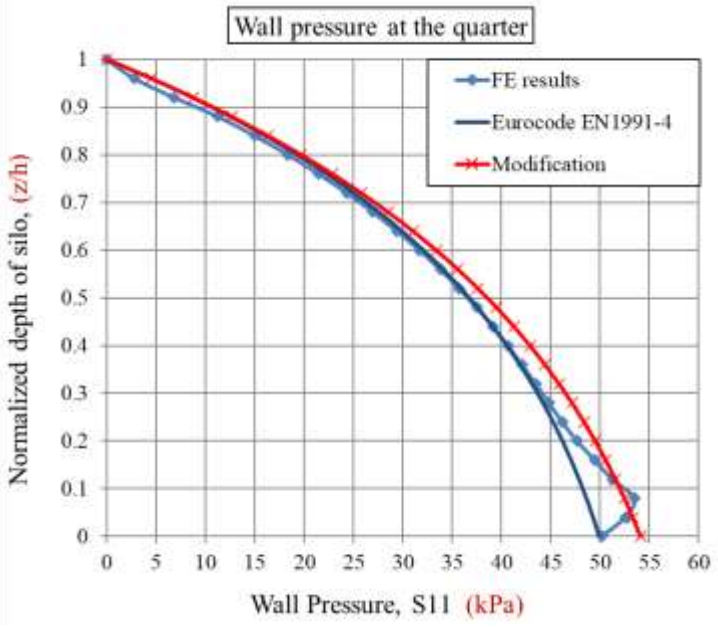

(c)

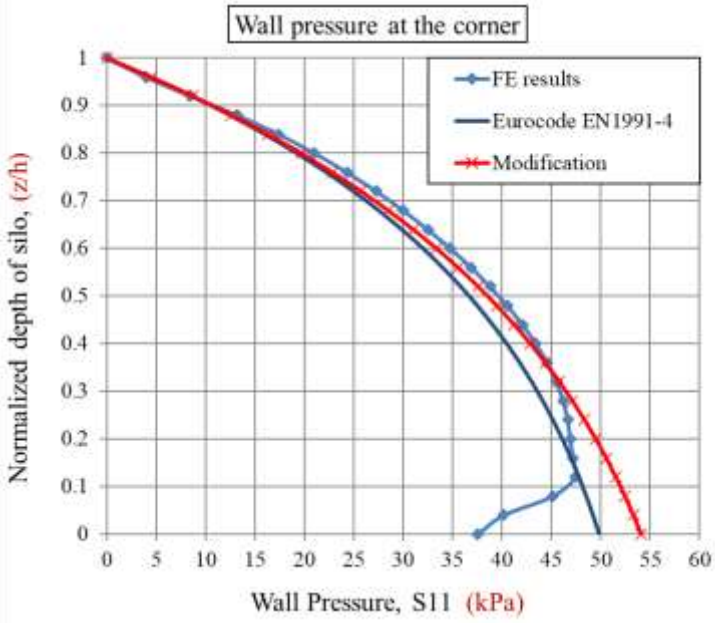

Figure 18. Comparison of the modified Janssen approach, the current Eurocode approach, and the FE results, (a) at the middle, (b) at the quarter, (c) at the corner [h/a= 2.5]

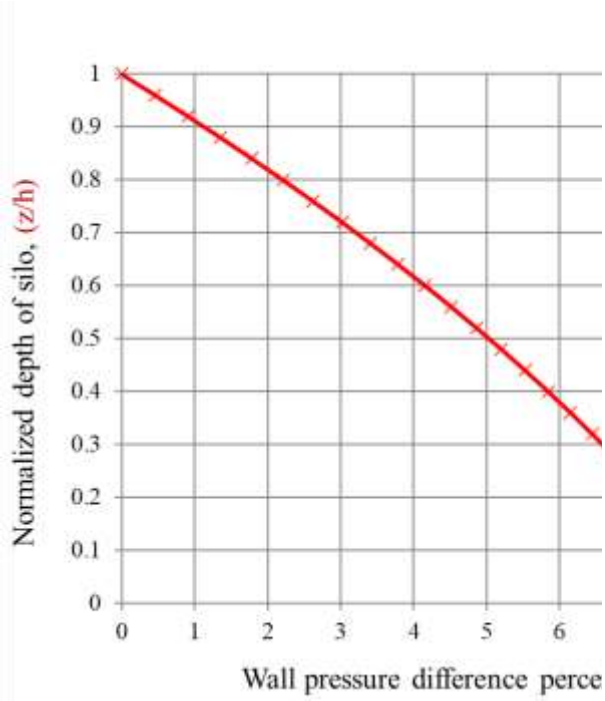

Figure 19 give the same information about the variation of the normalized difference percentage concerning the general shape and position of the maximum and lowest wall pressure difference percentages. The normalized difference percentage in the slender silo is greater than that in the squat silo throughout the silo height. The highest normalized difference in the slender silo is 8.5%, whereas it is 6.4% in the squat silo.

Table 6 displays the calculation and tabulation of the vertical load applied to the wall using both approaches. The transmitted vertical wall loads were estimated using the parameters in Section 3.5.2 for the proposed approach. The compressive vertical wall loads for the proposed technique in the slender are comparable to those of squat silos, which is roughly around 4%, which might reduce the wall thickness estimate. The procedure for calculating the subsequent terms is shown in Section 3.3.

(a)

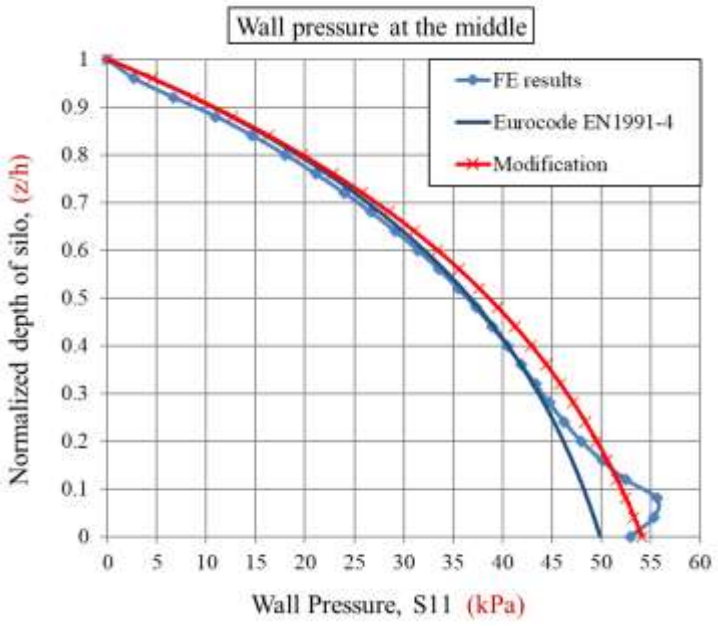

(b)

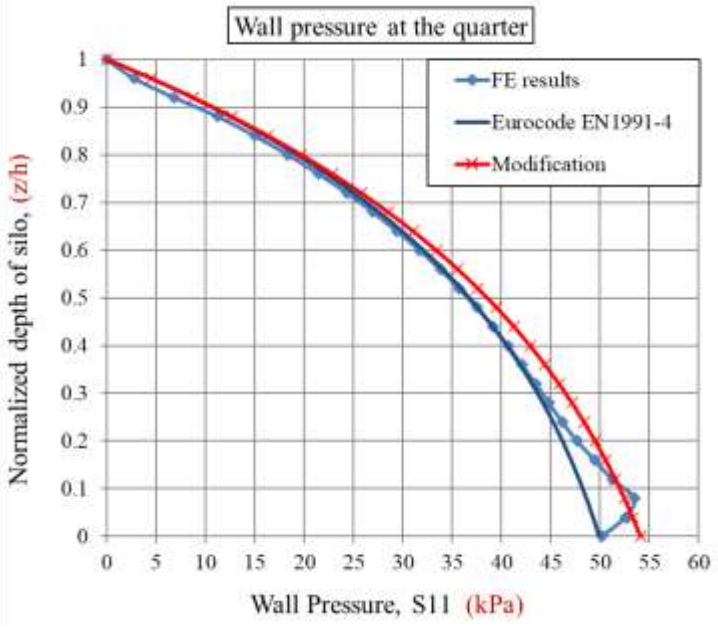

(c)

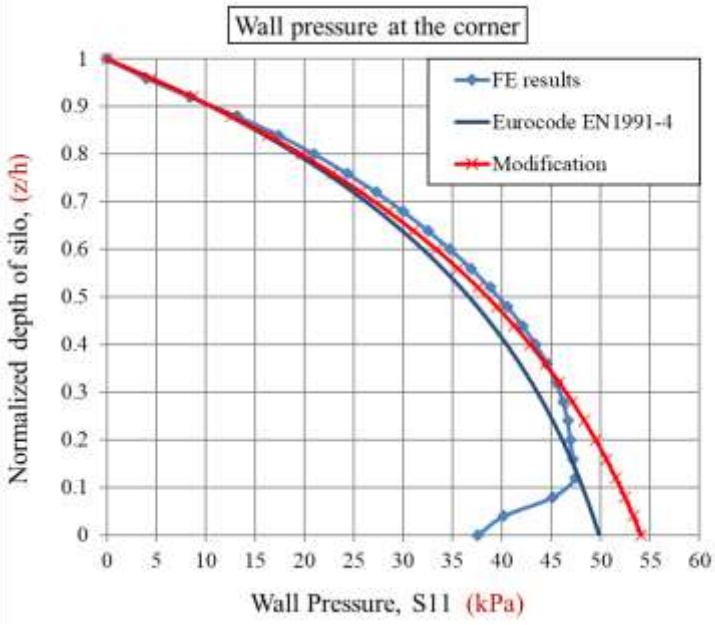

Figure 18. Comparison of the modified Janssen approach, the current Eurocode approach, and the FE results, (a) at the middle, (b) at the quarter, (c) at the corner [h/a= 2.5]

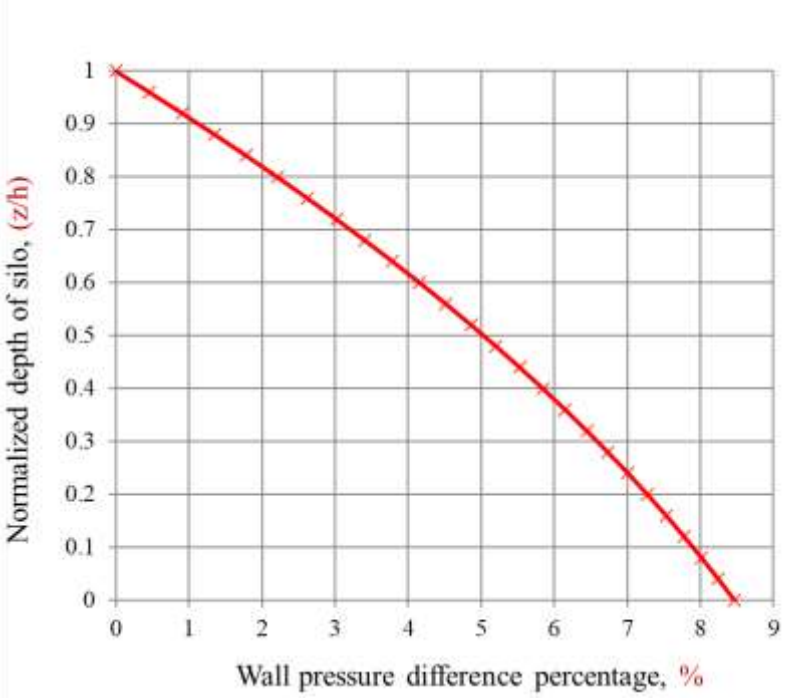

Figure 19. The normalized difference percentage of wall pressure between the modified and the existing Eurocode approaches for a slender silo

Table 6. Comparison of the vertical loads transferred to the walls by the two approaches

No.	Parameter	The existing approach	The proposed approach
1	The hydraulic radius, R (m)	1.605	1.811
2	the specific weight of the material, ω (kg/m^3)	1587	1587
3	Wall friction coefficient, μ	0.445	0.445
4	The lateral pressure ratio, λ	0.4628	0.4628
5	The depth from the free surface, Z (m)	16	16
6	The maximum lateral wall pressure, $\boldsymbol{P_x}$ (kPa)	49.9	54.11
7	The maximum vertical pressure on the base, $\boldsymbol{P_v}$ (kPa)	107.8	116.92
8	Total vertical loads (Bulk solids, MN)	10.47	10.47
9	The vertical load on the base (MN)	4.44	4.82
10	The vertical load supported by the silo wall (MN)	6.03	5.65
11	The percentage of the transferred load to the wall	57.5 %	54 %

4. Discussion

The Janssen equation is currently the most widely used approach for predicting wall pressure for silos in several design codes and standard tests [6,7,11,12,27,28]. However, the Janssen has several limitations as the equation was derived initially for circular rigid silos. Therefore, applying such an equation for noncircular silos gives inaccurate results.

This study shows that wall stiffness significantly impacts pressure distribution throughout the silo wall. As a result, the primary goal of this research was to find a unitless factor, *i* = a/t," that can successfully distinguish between rigid and flexible walls.

The results demonstrate that the FEM with a value of [a/t ≤ 25] can offer a perfect rigid silo behavior, and the code can be applied directly for such cases. Meanwhile, the FEM with a value of [a/t =45] can successfully represent the case of relatively rigid wall silos in terms of three critical criteria: uniform pressure distribution throughout the silo wall, acceptable wall deformation, and vertical load capacity of these walls. Consequently, the authors propose this value as the conservative wall width-to-thickness ratio (*i*) that meets the wall rigidity case. Moreover, it offers the solution when finite element modeling is essential or when the square silo wall must be strengthened to change from flexible to stiff behavior. As a result, the code applicability can be determined based on the outcomes.

Furthermore, a proposed approach was developed based on the Janssen equation for the square silo. Due to the missing shade regions in the square section when considered circular, the maximum wall pressure for the silo wall cannot be predicted using the Janssen equation. According to the results, the proposed new approach gives a better prediction of the maximum wall pressure since it is based on the same volume concept. It is important to mention that the proposed approach can be applied to both squat and slender silo walls.

5. Conclusion

This study employed a validated 3-D FEM to investigate the effect of the wall width-to-thickness ratio (*i*) on the lateral wall pressure for thin-walled steel silos. Analysis of results obtained for many silo models led to the following remarks:

The finite element results showed that the wall width-to-thickness ratio substantially influences the lateral wall pressure in silos. The influence of wall width-to-thickness ratio on wall pressure distribution, lateral displacement, and vertical load capacity of these walls was investigated and compared to rigid wall analysis results using the Janssen method. For steel silos, it is found that a wall width-to-thickness ratio (a/t) of less than 25 produces results fairly similar to rigid silo behavior, while walls with (a/t) values of up to 45 can be treated as rigid with accuracy good enough for practical designs. The authors recommended the later ratio to silo designers as a minimum to guarantee wall stiffness for unstiffened, square steel silos.

For square silos, the authors proposed a new approach for calculating the radius of equivalent circular silos based on an equal volume concept. In comparison to Eurocode, which uses the concept of hydraulic radius, the proposed new approach presented above was shown to be more accurate. A good characteristic of the proposed modification is its simplicity, which improves accuracy without complicating calculations.

Eventually, structural engineers can employ the findings from this study to decide whether a steel silo wall is rigid or flexible and to predict the behavior of flexible-wall steel silos. Besides, the findings of this research can be utilized to improve silo design codes and standards.

References

[1] A. Juan, J.M. Moran, M.I. Guerra, A. Couto, F. Ayuga, P.J. Aguado, Establishing stress state of cylindrical metal silos using finite element method: Comparison with ENV 1993, Thin-Walled Structures. 44 (2006)

1192–1200. https://doi.org/ 10.1016/ j.tws.2006.09.001.

[2] C. Sonat, C. Topkaya, J.M. Rotter, Buckling of cylindrical metal shells on discretely supported ring beams, Thin-Walled Structures. 93 (2015) 22–35. https://doi.org/ 10.1016/j. tws. 2015.03.003.

[3] H. Jing, H. Chen, J. Yang, P. Li, Shaking table tests on a small-scale steel cylindrical silo model in different filling conditions, Structures. 37 (2022) 698–708. https://doi.org/10.1016/j.istruc.2022.01.026.

[4] A. Hilal, A.M. Sanad, M.H. Abdelbarr, O.M.O. Ramadan, H.A. Abdalla, Three-Dimensional Finite Element Analysis for Pressure on Flexible Wall Silos, Applied Sciences. 12 (2022) 9251. https://doi.org/10.3390/app12189251.

[5] K. Rejowski, P. Iwicki, J. Tejchman, M. Wójcik, Buckling resistance of a metal column in a corrugated sheet silo-experiments and non-linear stability calculations, Thin-Walled Structures. 182 (2023) 110206. https://doi.org/10.1016/j. tws.2022.110206.

[6] A.J. Matchett, A principal stress cap model for stresses in square silos, with some examples of exponential stress, Powder Technology. 412 (2022) 117983. https://doi.org/10. 1016/j.powtec.2022.117983.

[7] R.J. Goodey, C.J. Brown, J.M. Rotter, Rectangular steel silos: Finite element predictions of filling wall pressures, Engineering Structures. 132 (2017) 61–69. https://doi.org/ 10.1016/j.engstruct.2016.11.023.

[8] J.M. Rotter, R.J. Goodey, C.J. Brown, Towards design rules for rectangular silo filling pressures, Engineering Structures. 198 (2019) 109547. https://doi.org/10.1016/j. engstruct.2019.109547.

[9] C.J. Brown, J. Nielsen, Silos: Fundamentals of Theory, Behaviour and Design, CRC Press, 1998.

[10] H.A. JANSSEN, Versuche uber Getreidedruck in Silozellen, Z. Ver. Dtsch. Ing. 39 (1895) 1045–1049. https://ci.nii.ac. jp/naid/10029334428/ (accessed March 20, 2022).

[11] EN 1991 –4. Eurocode 1-actions on structures-part 4: silos and tanks 2006 European Standard. European Committee for Standardization Brussels., (n.d.).

[12] ACI 313. American Concrete Institute. Design specification for concrete silos and stacking tubes for storing granular materials and commentary American Concrete Institute; 2016., (n.d.).

[13] AS 3774-1996, Loads on bulk solids containers, Standards Australia, Homebush, NSW, Oct. 1996., (n.d.).

[14] J.Y. Ooi, J.M. Rotter, Wall pressures in squat steel silos from simple finite element analysis, Computers & Structures. 37 (1990) 361–374. https://doi.org/10.1016/0045-7949(90)90026-X.

[15] R.J. Goodey, C.J. Brown, J.M. Rotter, Verification of a 3-dimensional model for filling pressures in square thin-walled silos, Engineering Structures. (2003) 11.

[16] R.J. Goodey, C.J. Brown, J.M. Rotter, Predicted patterns of filling pressures in thin-walled square silos, Engineering Structures. (2006) 11.

[17] E. Ragneau, J.-M. ARIBERT, A.M. Sanad, Modèle tri-dimensionnel aux éléments finis pour le calcul des actions sur les parois d'un silo (remplissage et vidange), Construction Métallique. (1994) 3–25.

[18] A.M. Sanad, J.Y. Ooi, J. Holst, J.M. Rotter, Computations of granular flow and pressures in a flat-bottomed silo, Journal of Engineering Mechanics. 127 (2001) 1033–1043.

[19] C.J. Brown, E.H. Lahlouh, J.M. Rotter, Experiments on a square planform steel silo, Chemical Engineering Science. 55 (2000)

4399–4413. https://doi.org/10. 1016/ S0009-2509(99)00574-6.

[20] E.H. Lahlouh, C.J. Brown, J.M. Rotter, Loads on rectangular planform steel silos, department of civil and environmental engineering, the university of Edinburgh, 1995.

[21] J.M. Rotter, C.J. Brown, E.H. Lahlouh, Patterns of wall pressure on filling a square planform steel silo, Engineering Structures. (2002) 16.

[22] DS Simulia. Abaqus/CAE user's manual; 2013, (n.d.).

[23] R.J. Goodey, Rectangular silos; Interaction of structure and stored bulk solid, Thesis, Brunel University School of Engineering and Design PhD Theses, 2002. http://bura.brunel.ac.uk/handle/2438/5246 (accessed April 24, 2022).

[24] EN1993-4-1 (2007) (English): Eurocode 3: Design of steel structures, Part 4 – 1: Silos., (n.d.).

[25] Y. Ma, R. Bai, L.-P. Yang, H.-X. Yang, S.-D. Guo, Coupling effects of the different temperature patterns and storage pressures on the buckling of a steel silo, Structures. 36 (2022) 168–188. https://doi.org/10.1016/ j.istruc. 2021. 12.002.

[26] A.M. Mehretehran, S. Maleki, Axial buckling of imperfect cylindrical steel silos with isotropic walls under stored solids loads: FE analyses versus Eurocode provisions, Engineering Failure Analysis. 137 (2022) 106282. https://doi.org/10. 1016 /j. engfailanal. 2022.106282.

[27] J.M. Rotter, Guide for the economic design of circular metal silos, CRC press, 2001.

[28] S.S. Safarian, Design and construction of silos and bunkers, Van Nostrand Reinhold, New York, 1985.